



K asteroids and CO3/CV3 chondrites

T. H. BURBINE¹*, R. P. BINZEL², S. J. BUS² AND B. E. CLARK³

¹Department of Mineral Sciences, National Museum of Natural History, Smithsonian Institution, Washington D.C. 20560-0119, USA

²Department of Earth, Atmospheric, and Planetary Sciences, Massachusetts Institute of Technology, Cambridge, Massachusetts 02139, USA

³Center for Radiophysics and Space Research, Cornell University, Ithaca, New York 14853, USA

*Correspondence author's e-mail address: burbine.tom@nmnh.si.edu

(Received 2000 June 28; accepted in revised form 2000 October 3)

Abstract—Reflectance spectra from 0.44 to 1.65 μm were obtained for three K asteroids. These objects all have spectra consistent with olivine-dominated assemblages whose absorption bands have been suppressed by opaques. The two observed Eos family members (221 Eos and 653 Berenike) are spectral analogs to the CO3 chondrite Warrenton. The other observed object (599 Luisa) is a spectral analog for CV3 chondrite Mokoia. These asteroids are all located near meteorite-supplying resonances with the Eos family cut by the 9:4 resonance and Luisa is found near the 5:2 resonance. However, K asteroids have been identified throughout the main belt so it is difficult to rule out other possible parent bodies for the CO3 and CV3 chondrites.

INTRODUCTION

The major goal of asteroid spectroscopy is the linkage of meteorites and asteroids and, through this process, the placement of meteorites into a geologic context. This goal is best accomplished when a match is found between the laboratory spectra of a meteorite and the telescopic spectrum of an asteroid. However, even when a match is established, it is worth reassessing in the light of spectra with increased sensitivity or spectral range. In this paper, we look at the proposed match between K asteroids and CO3/CV3 carbonaceous chondrites, which have been linked by previous workers, but for which we have new asteroid spectra.

Bell (1988) proposed the K class on the basis of near-infrared observations (Bell *et al.*, 1988) of a number of objects in the Eos family. K asteroids were provisionally defined as having visual albedos near 0.09, S-like spectral curvature at visual wavelengths, weak 1 μm features, and relatively flat reflectances from 1.1 to 2.5 μm . The observed Eos family members were noted to have visible and near-infrared spectra similar to CO3/CV3 chondrites (Fig. 1); however, the near-infrared spectra of these asteroids were rather noisy with a large amount of scatter, which prohibits accurate analysis of their compositions. The taxonomies of Tedesco *et al.* (1989) and Bus (1999) identified K asteroids on the basis of their visible spectra. Both studies found these objects within the Eos family and throughout the belt.

Eos family members have been known since the work of Gradie and Zellner (1977) to have spectra and albedos intermediate between C and S objects. Veeder *et al.* (1995)

found that Eos family members had broadband colors in the near-infrared consistent with the observed objects having similar surface compositions.

The Eos family contains over 450 objects (Zappalà *et al.*, 1995). Visible charge coupled device (CCD) spectra of 45 asteroids in the Eos family by Doressoundiram *et al.* (1998) show a continuum of spectral properties for almost all objects with only two observed asteroids seeming to be interlopers. Many of their observed objects had spectral properties similar to CO3/CV3 chondrites; however, other compositions could not be ruled out due to the limited wavelength range (0.48 to 0.92 μm) of their spectra. Near-infrared spectra are vital for interpreting asteroid compositions since minerals such as olivine and pyroxene have absorption features that extend past 1 μm . During a pre-proposal assessment of visible and near-infrared data for 221 Eos, Clark (pers. comm.) noted similarities between Eos and CO3 chondrites.

CO3 and CV3 carbonaceous chondrites are both composed primarily of chondrules within a dark matrix (*e.g.*, Dodd, 1981; Brearley and Jones, 1998). The chondrules in these meteorites tend to be predominately olivine. CV3 chondrites typically contain larger volume percentages of matrix (~30–40% for CO chondrites and ~35–50% for CV chondrites) (*e.g.*, Grossman *et al.*, 1988; Brearley and Jones, 1998). Both types contain roughly similar chondrule abundances (~35–40% for CO chondrites and 35–45% for CV chondrites). Relative to CO3 chondrites, CV3 chondrites tend (McSween, 1977; Dodd, 1981) to have larger chondrules (0.5–2 mm versus sizes less than 0.5 mm in CO3 chondrites). CV chondrites also tend to have a

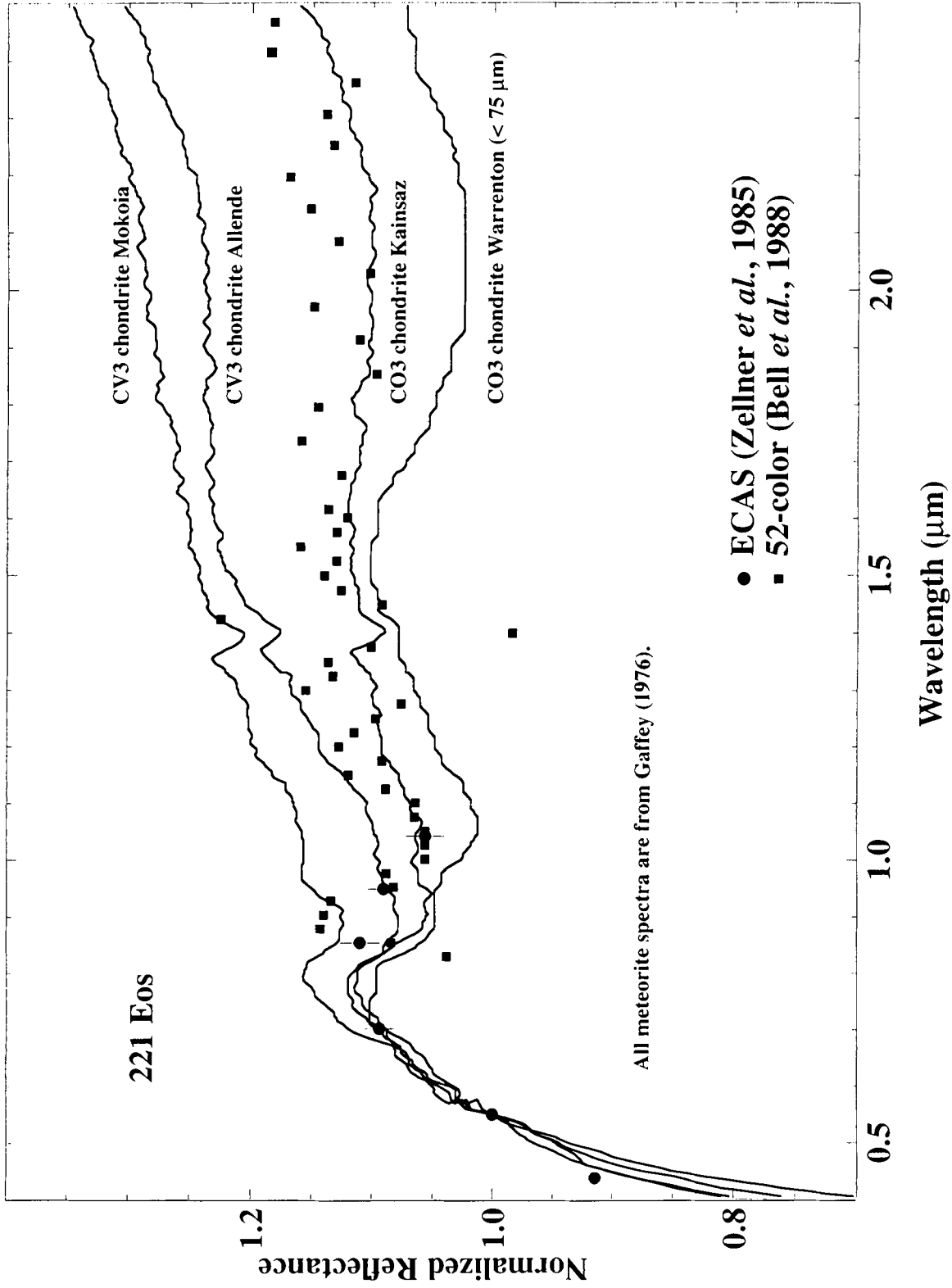


FIG. 1. Reflectance spectrum of K asteroid 221 Eos versus spectra (Gaffey, 1976) of CO3 chondrite Kainsaz, CO3 chondrite Warrenton (particle size less than 75 μm), CV3 chondrite Allende, and CV3 chondrite Mokoia. The spectra of the Allende and Mokoia samples were measured for particulate samples with grain sizes between approximately 30 and 300 μm . The dark circles are eight-color asteroid survey (ECAS) data (Zellner *et al.*, 1985) and the dark squares are 52-color data (Bell *et al.*, 1988). All spectra are normalized to unity at 0.55 μm . Error bars are $\pm 1\sigma$. No error bars are given for the 52-color data since only one set of observations were taken.

higher abundance of calcium-aluminum-rich inclusions (CAIs) than CO chondrites. The matrices of CO3 and CV3 chondrites tend to be dominated by fine-grained olivine plus accessory phases such as phyllosilicates and opaques (*e.g.*, metallic iron, magnetite). Both types of meteorites are petrologic type 3, indicating little to no recrystallization.

CO3 chondrites are subdivided (Scott and Jones, 1990) into a metamorphic sequence of petrologic types 3.0 to 3.7 with the amount of thermal metamorphism increasing with increasing number. Scott and Jones (1990) believe that the metamorphic trends found among these meteorites are consistent with all CO3 chondrites coming from the same parent body. The CV3 chondrites also have been divided into a number of subgroups (McSween, 1977; Weisberg *et al.*, 1997; Krot *et al.*, 1998) using differences in opaque mineralogies and degrees of aqueous alteration. Krot *et al.* (1998) argues that the presence of a variety of lithologies from different subgroups in some CV3 chondrite breccias are consistent with all CV3 chondrites coming from one heterogeneously altered object.

An important question concerning K asteroids is whether or not higher resolution spectral studies will confirm or refute their proposed linkage to the CO3/CV3 chondrites. Previous near-infrared studies of these objects have produced only low-quality (Bell *et al.*, 1988) or low-resolution data (Clark *et al.*, 1995; Veeder *et al.*, 1995), which makes any mineralogical interpretations difficult. To help determine their compositions, three of these objects (221 Eos, 599 Luisa, and 653 Berenike) (Table 1) were observed with wavelength coverage of 0.44 to 1.65 μm . All of these asteroids have relatively large diameters (39 to 104 km). Eos and Berenike are both in the Eos family as defined by Zappalà *et al.* (1995).

OBSERVATIONAL TECHNIQUES

The visible CCD asteroid spectra were taken by Bus (1999) at the 2.4 meter telescope at the Michigan-Dartmouth-MIT (MDM) observatory at Kitt Peak in Arizona as part of the second stage of the small main-belt asteroid spectroscopic survey (SMASS II). Data acquisition procedures and data reduction techniques are described in Bus (1999). The usable wavelength coverage of SMASS II is from 0.44 to 0.92 μm . The data cut off at the telluric water band, which is centered near 0.94 μm . The data have 1σ error bars for individual points.

TABLE 1. Orbital characteristics of the K asteroids.

Asteroid	a (AU)	e'	$\sin i'$	Diameter (km)	HCM Family
221 Eos	3.012	0.077	0.173	104	Eos
599 Luisa	2.773	0.228	0.288	65	
653 Berenike	3.014	0.080	0.181	39	Eos

Proper elements (a , e' , $\sin i'$) are from Knežević and Milani (1994). The semimajor axes (a) are given in astronomical units (AU). Diameters (km) are from infrared astronomical satellite (IRAS) observations (Tedesco, 1994). HCM (hierarchical cluster method) family designations are from Zappalà *et al.* (1995).

The near-infrared CCD spectra were taken as part of the small main belt asteroid survey in the near-infrared (SMASSIR) (Burbine, 2000) at the infrared telescope facility (IRTF), which is located at Mauna Kea on the island of Hawai'i. A low-resolution "asteroid" grism developed by Richard Binzel with appropriate blocking filters is used to record a simultaneous first-order spectrum from ~ 0.90 to 1.65 μm with a dispersion of ~ 0.015 μm per pixel on the NASA space infrared telescope facility camera (NSFCAM) InSb array. The wavelength calibration was obtained by taking spectral images of the flatly-illuminated dome through a number of narrow band filters. The SMASSIR wavelengths overlap the visible CCD coverage of SMASS II. Spectral coverage past ~ 1.65 μm is not possible due to the overlap of a second-order spectrum.

Observational parameters for the SMASSIR spectra plotted in this paper are given in Table 2. Each asteroid spectrum is divided by a standard (solar analog) star spectrum observed at a similar airmass and time. This division by the standard star spectrum produces the reflectance spectrum for each asteroid relative to the Sun.

Multiple images are taken for each asteroid and standard star. Images are obtained in pairs (images "A" and "B") where the spectra fall on alternating parts of the CCD chip. As much as possible, the "A" image is repeatedly placed on the same column (and similarly for the "B" image). Image "A" is subtracted by "B" and *vice versa* to remove background counts from the sky in each image. Spectral data reduction was done using the Image Reduction and Analysis Facility (IRAF),

TABLE 2. Observational parameters for the SMASSIR observations of the K asteroids.

Asteroid	Date	Time (UT)	Airmass	Images	Standard Star	Airmass
221 Eos	29/04/98	10:43–11:01	1.06	10	102-1081	1.07
599 Luisa	02/05/98	08:32–08:42	1.04	6	102-1081	1.08
653 Berenike	04/01/98	13:14–13:29	1.05	10	Hyades 64	1.05

Dates (day/month/year) and times of the observations are given in universal time (UT). The number of images is the number of exposures that were used in the reduction of the asteroid spectrum. Standard star 102-1081 is from the Landolt (1973) listing of UVB (ultraviolet, blue, visible) standard stars. The quoted airmass is the average airmass for the set of observations.

developed by the National Optical Astronomical Observatories. The IRAF package *apall* was used to produce a spectrum from each image by summing the pixel values within a specified aperture at each point along the dispersion axis and subtracting any remaining background level.

Since the different parts of the CCD chip may have different sensitivities, spectra from each image from the "A" side of the chip are combined to produce a composite "A" spectrum for a particular object, and similarly for the "B" side spectra. The composite asteroid spectrum from the "A" side is divided by the spectrum of the composite standard star from the "A" side, and similarly for the "B" side spectra. The "A" and "B" reflectance spectra are combined to produce the final reflectance spectrum for a particular night.

An atmospheric water band centered near $1.4 \mu\text{m}$ causes the points between 1.35 and $1.5 \mu\text{m}$ to be very suspect and not usable for most asteroids. Due to the problems in correcting for atmospheric water, no corrections to the spectra have been made and points that appear to have been affected significantly have been deleted. Weaker atmospheric effects are also sometimes present in the spectra at ~ 0.94 and $\sim 1.15 \mu\text{m}$.

The average uncertainty in the spectral slope for an asteroid spectrum at the SMASSIR wavelengths is on the order of 5%, which is comparable to slope uncertainties in the visible (Bus, 1999). Eos was observed six separate times (Burbine, 2000) and its spectral properties were very repeatable. Only the spectrum of Eos from 29/04/98, which has the lowest residual atmospheric water feature at $\sim 1.4 \mu\text{m}$ of all of the Eos observations, is plotted since this spectrum should be the least affected by the atmosphere.

One-sigma error bars for the reflectance values were calculated using Poisson statistics. The signal-to-noise ratio for each image was calculated by dividing the signal (the summed pixel values with the remaining background level removed from the subtracted images) by the noise (the square root of the summed pixel values with no remaining background level removed from the unsubtracted images). The inverse of the signal-to-noise is the fractional error for each image. The fractional errors for each image (standard star and asteroid) could be propagated to produce the 1σ error bars for the final composite spectra.

Each SMASSIR spectrum was normalized to a visible spectrum. The normalization to the visible spectrum was done by first fitting the SMASSIR spectrum with errors using a cubic spline program (Reinsch, 1967) that was adapted by Schleicher (pers. comm.) and has been previously used by Bus (1999). Points that appeared significantly affected by atmospheric water features were not used in the fit. The SMASSIR spectra were fit from 0.92 to $1.65 \mu\text{m}$ at $0.01 \mu\text{m}$ intervals. The $0.92 \mu\text{m}$ endpoint was chosen since the SMASS II spectra were fit from 0.44 to $0.92 \mu\text{m}$ (Bus, 1999) and the two fits could be directly overlapped. Also, the number of counts measured shortward of $0.92 \mu\text{m}$ in SMASSIR is rapidly decreasing, which increases the uncertainty in the value of those points. The SMASSIR fit

was then normalized to the fitted visible spectrum. The actual SMASSIR spectrum was multiplied by this normalization factor and then overlaid on the SMASS II spectrum to get the best continuous spectrum from 0.44 to $1.65 \mu\text{m}$.

All meteorite spectra plotted in this paper are from Gaffey (1976) and have had a correction factor of $+0.025 \mu\text{m}$ added to their original wavelengths to compensate for a later-discovered calibration offset (Gaffey, 1984).

ANALYSIS

All three observed objects are plotted (Fig. 2) versus a number of CO3 and CV3 chondrites, which have been suggested to be the best spectral analogs to the K asteroids (*e.g.*, Bell, 1988). The spectra of CO3 and CV3 chondrites can be seen to have very diverse spectral properties. Johnson and Fanale (1973) found that the continuum slopes for the spectra of CO3 and CV3 chondrites tend to increase (or redden) as the particle size decreases. Also, the CO3 chondrites almost always have stronger $1 \mu\text{m}$ absorption features than CV3 chondrites, which is most likely due to the CV3 chondrites containing a higher abundance of the dark matrix. The opaque nature of the dark matrix material tends to suppress the absorption features due to mafic minerals such as olivine. The best spectral matches to these particular objects are plotted separately for clarity (Fig. 3). Other meteorite types (*e.g.*, ordinary chondrites, CI chondrites, CM chondrites, eucrites) are poor spectral matches to these objects.

The two Eos family members (Eos and Berenike) (Fig. 2) can be seen to be almost perfect spectral matches with each other in the visible and near-infrared. Both have ultraviolet (UV) features with similar strengths, plus an absorption feature with a band depth of $\sim 10\%$ centered around 1.06 – $1.08 \mu\text{m}$. The wavelength position of this feature plus the more subtle features at ~ 0.9 and $\sim 1.3 \mu\text{m}$ indicates an olivine-rich assemblage where the olivine bands are suppressed in strength due to an opaque (*e.g.*, metallic iron, sulfide, carbon).

These two spectra (Eos and Berenike) are remarkably similar (Fig. 3) to spectra of CO3 chondrite Warrenton. (The second best match to Eos and Berenike from Fig. 2 appears to be CO3 chondrite Ormans.) Warrenton was classified as a type 3.6 CO chondrite by Scott and Jones (1990), indicating that Warrenton experienced a higher degree of thermal metamorphism compared to other CO3 chondrites. The two Eos family members fall intermediate between a Warrenton spectrum for a particle size less than $75 \mu\text{m}$ and one between 75 and $150 \mu\text{m}$. The Warrenton spectra have a similarly shaped absorption feature due to olivine that is centered at $1.06 \mu\text{m}$. Warrenton is 75% vol% olivine (Fa₂₇; Scott and Jones, 1990), 4% pyroxene, 6% metallic iron, and 5% troilite (Wahl, 1950). The chondrules and matrix (Keller and Buseck, 1990) are both dominated by olivine. The albedo of Eos (0.14 ± 0.01) (Table 3) falls intermediate between the albedos (0.10 and 0.16) of the Warrenton spectra, while Berenike is brighter (albedo of 0.24 ± 0.03). Berenike's higher albedo could imply a finer-

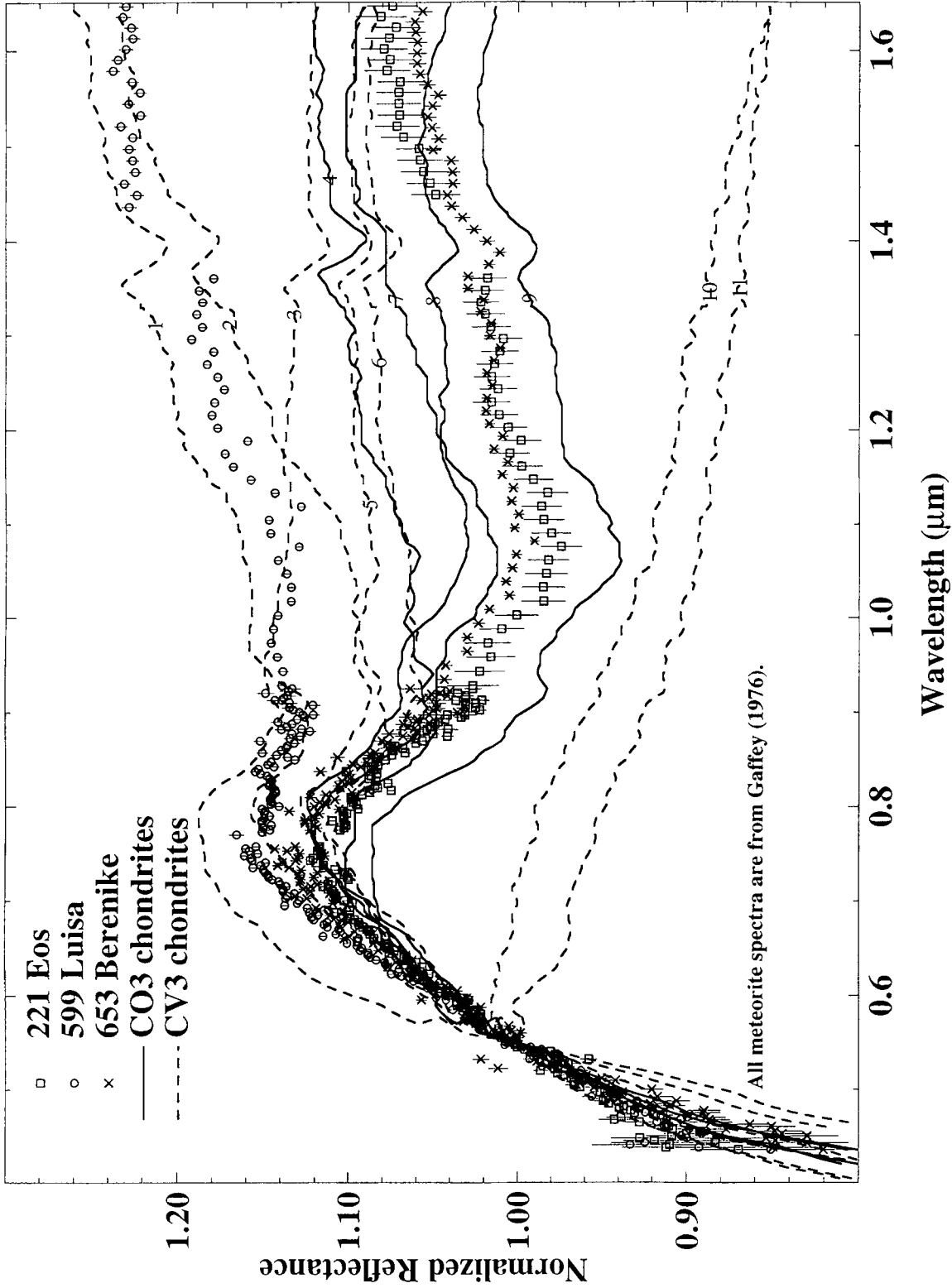


FIG. 2. Reflectance spectra for K asteroids 221 Eos (squares), 599 Luisa (circles), and 653 Berenike (crosses) versus spectra (Gaffey, 1976) of CO3 (filled lines) and CV3 (dashed lines) chondrites. Each meteorite spectrum is numbered according to decreasing reflectance at 1.3 μm . The order is (1) Mokoia (CV3), (2) Allende (CV3), (3) Leoville (CV3), (4) Kainsaz (CO3), (5) Grosnaja (CV3) (particle size less than 75 μm) (6) Vigarano (CV3), (7) Warrenton (CO3) (less than 75 μm), (8) Ormans (CO3), (9) Warrenton (CO3) (between 75 and 150 μm), (10) Grosnaja (CV3) (between 150 and 500 μm), and (11) Grosnaja (CV3) (between 75 and 150 μm). Meteorite samples where the grain size is not explicitly noted were measured for particulate samples with grain sizes between approximately 30 and 300 μm . Visible asteroid spectra (0.44 to 0.92 μm) are from SMASS II (Bus, 1999) and near-infrared spectra (\sim 0.90 to 1.65 μm) are from SMASSIR (Burbine, 2000). All spectra are normalized to unity at 0.55 μm . Error bars are $\pm 1\sigma$.

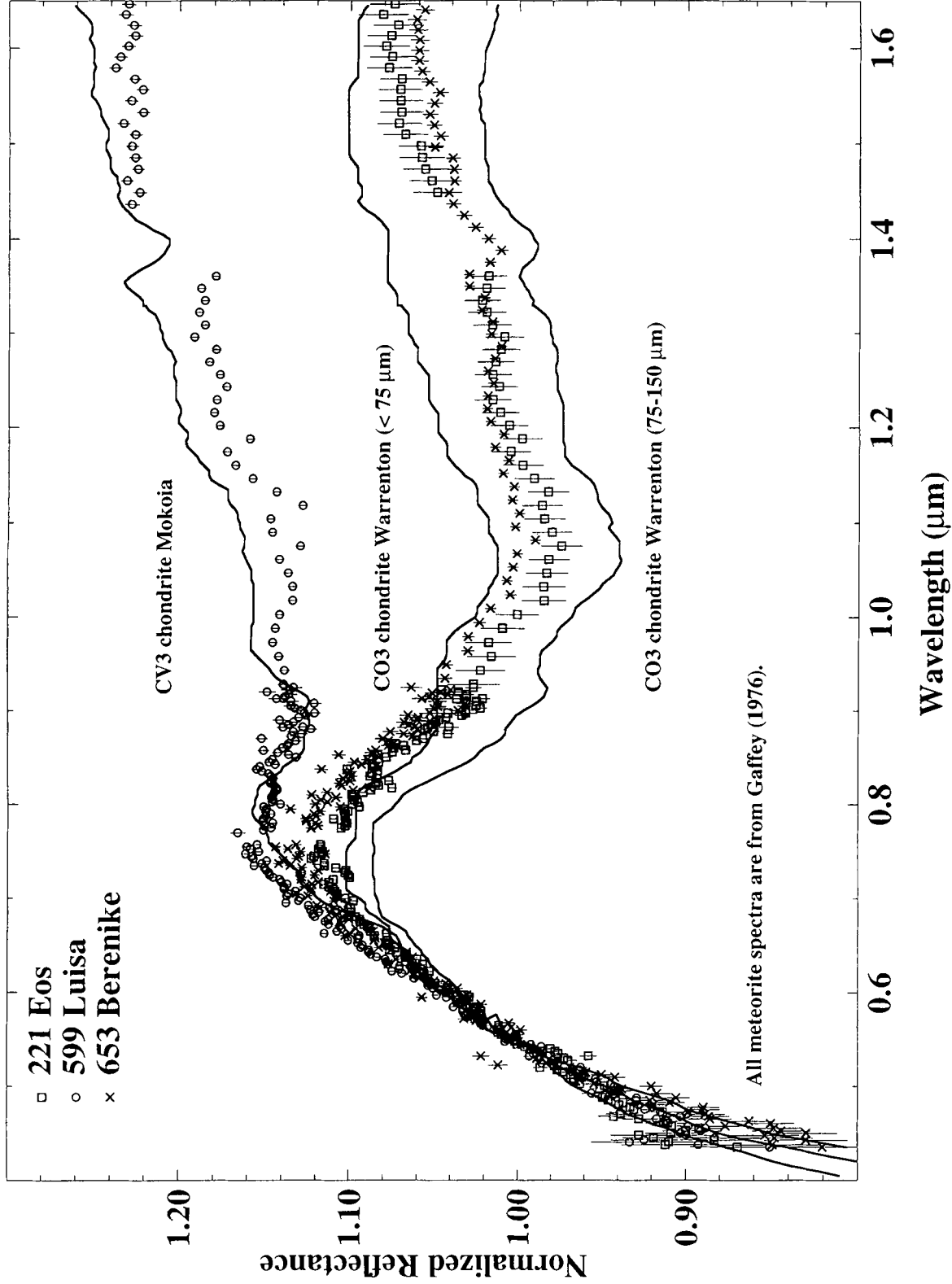


FIG. 3. Reflectance spectra for K asteroids 221 Eos (squares), 599 Luisa (circles), and 653 Berenike (crosses) versus spectra (Gaffey, 1976) of CV3 chondrite Mokoia and CO3 chondrite Warrenton (particle sizes less than 75 μm and between 75 and 150 μm). Eos and Berenike have spectra similar to Warrenton and Luisa has a spectrum similar to Mokoia. The spectrum of the Mokoia sample was measured for a particulate sample with grain sizes between approximately 30 and 300 μm . Visible asteroid spectra (0.44 to 0.92 μm) are from SMASS II (Bus, 1999) and near-infrared spectra (\sim 0.90 to 1.65 μm) are from SMASSIR (Burbine, 2000). All spectra are normalized to unity at 0.55 μm . Error bars are $\pm 1\sigma$.

grained surface and/or a lower amount of opaques than Eos or the Warrenton samples; however, the similarities in spectral properties between these three objects argues for similar compositions and particle sizes on their surfaces.

Luisa is redder (reflectances increase with increasing wavelength) (Fig. 2) than the two other K types. The scatter in the points makes any interpretation difficult, but an absorption feature centered at $\sim 1.1 \mu\text{m}$ is apparent in the spectrum. This feature is consistent with olivine that has had its band strength significantly suppressed by some type of opaque material. Luisa is spectrally similar to CV3 chondrite Mokoia (Fig. 3) with both spectra having weak absorption features centered at $1.1 \mu\text{m}$ and UV features of similar strengths. (The second best match to Luisa from Fig. 2 appears to be CV3 chondrite Allende.) In Mokoia, the mafic silicates are primarily fayalitic ($\text{Fa}_{>32}$) olivine (Weisberg and Prinz, 1998). Luisa is brighter (albedo of 0.14 ± 0.01) (Table 3) than the measured Mokoia sample (0.07). The albedos of other CV3 chondrites (Gaffey, 1976) vary from 0.06 to 0.11, which is closer to the albedo of Luisa.

Most of the CO3 and CV3 chondrites (including Warrenton and Mokoia) have a feature at $\sim 1.4 \mu\text{m}$ (Figs. 2 and 3). This feature is most likely due to bound water or structural OH in hydrated silicates or hydroxides (*e.g.*, King and Clark, 1989; Calvin and King, 1997) from pre-terrestrial aqueous alteration. Hydroxides from terrestrial alteration would also have a feature at this wavelength; however, Gaffey (1976) went to extensive lengths to try to eliminate the effects of terrestrial alteration in his spectra. All samples were checked for signs of visible alteration under a microscope and their spectra were also checked for alteration features (*e.g.*, a feature at $\sim 1.9 \mu\text{m}$, which is not present in the spectra of any of these CO3 or CV3 chondrites).

Hydrated silicates and hydroxides are commonly found in the matrices of CO3 and CV3 chondrites (*e.g.*, Brearley and Jones, 1998). This feature at $\sim 1.4 \mu\text{m}$ in the Mokoia spectrum is probably due to the presence of abundant phyllosilicates and Fe^{3+} -oxides (or hydroxides) in Mokoia (Tomeoka and Buseck, 1990). Transmission electron microscope (TEM) analyses of Warrenton (Keller and Buseck, 1990) do not show the presence of phyllosilicates, but Fe^{3+} -oxides (or hydroxides) were found. This feature at $\sim 1.4 \mu\text{m}$ in the Berenike spectrum is most likely due to an incomplete atmospheric correction of the observational data. Observations in the $3 \mu\text{m}$ wavelength region of Eos by Rivkin (1997) are consistent with Eos being anhydrous.

LINKING CO3/CV3 CHONDRITES TO K ASTEROIDS

Luisa is located near the 5:2 resonance at ~ 2.8 AU, which should be supplying fragments quickly into Earth-crossing orbits. Researchers (*e.g.*, Nesvorný and Morbidelli, 1998) have found that the lowest-order mean motion resonances (*e.g.*, 3:1, 5:2) tend to produce planet crossers on a much shorter timescale (a few Ma) compared to higher-order resonances (*e.g.*, 7:2, 9:4) (tens of Ma to about 1 Ga).

TABLE 3. Infrared astronomical satellite (IRAS) albedos (Tedesco, 1994) of the K asteroids and visual albedos (Gaffey, 1976) of the measured samples of the CO3 chondrite Warrenton and CV3 chondrite Mokoia.

Asteroid	IRAS albedo
221 Eos	0.14 ± 0.01
599 Luisa	0.14 ± 0.01
653 Berenike	0.24 ± 0.03
Meteorite	Visual albedo
Mokoia	0.07
Warrenton ($<75 \mu\text{m}$)	0.16
Warrenton (75 to $150 \mu\text{m}$)	0.10

The IRAS albedos are calculated using a thermal model. Albedos for the meteorites are their reflectances at $0.55 \mu\text{m}$. Particle sizes were specifically measured for the two Warrenton samples. The albedo of the Mokoia sample is for a particulate sample with grain sizes between approximately 30 and $300 \mu\text{m}$.

The Eos family is cut by the 9:4 resonance, which is located at ~ 3.03 AU (Morbidelli *et al.*, 1995). Zappalà *et al.* (2000) has identified a number of objects with spectra similar to Eos actually in the 9:4 resonance. Numerical simulations by Di Martino *et al.* (1997) found that $\sim 92\%$ of test particles that entered this resonance were ejected from the solar system. However, they believe that about 2% of all CO3/CV3 meteorites could be from the Eos family, due to the large amount of material that would enter the resonance during the event that created the family.

Interestingly, Mokoia (the best spectral analog to Luisa) has a relatively short cosmic-ray exposure age (9.7 Ma) while Warrenton (the best spectral analog for Eos and Berenike) has a much longer age (34 Ma) (Scherer and Schultz, 2000). Cosmic-ray exposure ages measure the time interval in space that a meteoroid spent exposed within a meter of the surface on its parent body or as a meter-sized object by determining the abundance of a cosmogenically-produced nuclide (*e.g.*, ^{21}Ne). The exposure ages for CO3 and CV3 chondrites range from about 1 to 63.5 Ma (Scherer and Schultz, 2000), which probably indicates that it is difficult for these meteorites to survive in space for hundreds of millions of years due to their relatively fragile nature. The measured carbonaceous chondrites with the oldest exposure ages (50.5 to 63.5 Ma) (Scherer and Schultz, 2000) are all CO3 chondrites; however, one CO3 chondrite did have an extremely young exposure age of 0.15 Ma.

The calculated ages for Mokoia and Warrenton (with error bars estimated to be less than 20%) appear roughly consistent with the locations of these objects in the belt. The 5:2 resonance (near Luisa) is believed to move fragments into Earth-approaching orbits on timescales of a few Ma (Nesvorný and Morbidelli, 1998). Di Martino *et al.* (1997) estimates that the

timescales for delivering fragments into Earth-crossing orbits from the 9:4 resonance (near the Eos family) are at least 50 Ma while Zappalà *et al.* (1998) has calculated timescales of 110–140 Ma, which are much longer than Warrenton's exposure age. The tendency for CO3 chondrites to have longer exposure ages than CV3 chondrites appears consistent with deriving CO3 chondrites from the Eos family and CV3 chondrites from Luisa. However, it is unclear if the large spread in exposure ages (Scherer and Schultz, 2000) for CO3 (0.15 to 63.5 Ma) and CV3 (1.4 to 31.5 Ma) chondrites is consistent with derivation from only one parent body for the CO3 chondrites and another for the CV3 chondrites.

Arguments trying to link these asteroids and meteorites are also related to the abundance of K asteroids in the asteroid belt and in the near-Earth population. Bus (1999) identified ~30 asteroids as K types; however, only about half of them are found in the Eos family with the rest scattered throughout the belt. Binzel (pers. comm.) has also identified a K asteroid (1999 JD₆) among the near-Earth asteroids. The non-uniqueness of this type of spectrum makes it difficult to rule out other possible parent bodies for these meteorites. Near-infrared studies of K asteroids are needed to ascertain if these objects are possible spectral analogs for CO3 and CV3 chondrites. Petrologic studies of CO3 (Scott and Jones, 1990) and CV3 chondrites (Krot *et al.*, 1998) appear consistent with all CO3 chondrites coming from one parent body and all CV3 chondrites coming from another. However, it is also impossible to definitively rule out multiple parent bodies for both the CO3 and CV3 chondrites from petrologic analyses of these meteorites.

CONCLUSIONS

The observed K asteroids are very good spectral matches from 0.44 to 1.65 μm for specific CO3 and CV3 chondrites, which is consistent with the interpretations of Bell (1988) and Doressoundiram *et al.* (1998) on the composition of K asteroids. The two Eos family members (221 Eos and 653 Berenike) are almost perfect spectral matches with each other. Their spectra also have the same absorption features due to olivine as CO3 chondrite Warrenton and fall between spectra of two particle sizes of this meteorite. The other observed K asteroid (599 Luisa) is a very good spectral match for CV3 chondrite Mokoia. K asteroids appear to have at least two distinct types of surface compositions. The cosmic-ray exposure ages of these two meteorites appear consistent with deriving these meteorites from these objects; however, a number of K asteroids have been identified throughout the belt so other possible parent bodies can not be ruled out.

Acknowledgments—Results from this paper were part of the Ph.D. thesis of T. H. B. at the Massachusetts Institute of Technology. Grants to R. P. B. (NASA grant NAG5-3939 and NSF grant AST-9530282) and B. E. C. (NASA grant NAG5-7892) supported this research. The authors would like to thank Dale Cruikshank for his review of the manuscript, Carlé Pieters for her work as associate editor, and Tim

McCoy for his very helpful comments. T. H. B. would also like to thank the people at the Center for Earth and Planetary Studies at the National Air and Space Museum of the Smithsonian Institution for the use of their Macintosh computers. T. H. B., R. P. B., S. J. B., and B. E. C. are visiting astronomers at the Infrared Telescope Facility, which is operated by the University of Hawai'i under contract to the National Aeronautics and Space Administration.

Editorial handling: C. M. Pieters

REFERENCES

- BELL J. F. (1988) A probable asteroidal parent body for the CV or CO chondrites (abstract). *Meteoritics* **23**, 256–257.
- BELL J. F., OWENSBY P. D., HAWKE B. R. AND GAFFEY M. J. (1988) The 52-color asteroid survey: Final results and interpretation (abstract). *Lunar Planet. Sci.* **19**, 57–58.
- BREARLEY A. J. AND JONES R. H. (1998) Chondritic meteorites. In *Planetary Materials* (ed. J. J. Papike), pp. 3-1–3-398. Reviews in Mineralogy, Mineralogical Society of America, Washington, D.C., USA.
- BURBINE T. H., JR. (2000) Forging asteroid-meteorite relationships through reflectance spectroscopy. Ph.D. thesis, Massachusetts Institute of Technology, Cambridge, Massachusetts, USA. 303 pp.
- BUS S. J. (1999) Compositional structure in the asteroid belt: Results of a spectroscopic survey. Ph.D. thesis, Massachusetts Institute of Technology, Cambridge, Massachusetts, USA. 367 pp.
- CALVIN W. M. AND KING T. V. V. (1997) Spectral characteristics of iron-bearing phyllosilicates: Comparison to Orgueil (C11), Murchison and Murray (CM2). *Meteorit. Planet. Sci.* **32**, 693–701.
- CLARK B. E., BELL J. F., FANALE F. P. AND O'CONNOR D. J. (1995) Results of the seven-color asteroid survey: Infrared spectral observations of ~50-km size S-, K-, and M-type asteroids. *Icarus* **113**, 387–402.
- DI MARTINO M., MIGLIORINI F., CELLINO A. AND ZAPPALÀ V. (1997) Can CO/CV meteorites come from the Eos family? (abstract). *Meteorit. Planet. Sci.* **32** (Suppl.), A35.
- DODD R. T. (1981) *Meteorites, A Petrologic-Chemical Synthesis*. Cambridge University Press, Cambridge, England. 368 pp.
- DORESSOUNDIRAM A., BARUCCI M. A., FULCHIGNONI M. AND FLORCZAK M. (1998) Eos family: A spectroscopic study. *Icarus* **131**, 15–31.
- GAFFEY M. J. (1976) Spectral reflectance characteristics of the meteorite classes. *J. Geophys. Res.* **81**, 905–920.
- GAFFEY M. J. (1984) Rotational spectral variations of asteroid (8) Flora: Implications for the nature of the S-type asteroids and for the parent bodies of the ordinary chondrites. *Icarus* **60**, 83–114.
- GRADIE J. AND ZELLNER B. (1977) Asteroid families: Observational evidence for common origins. *Science* **197**, 254–255.
- GROSSMAN J. N., RUBIN A. E., NAGAHARA H. AND KING E. A. (1988) Properties of chondrules. In *Meteoritics and the Early Solar System* (eds. J. F. Kerridge and M. S. Matthews), pp. 619–659. Univ. Arizona Press, Tucson, Arizona, USA.
- JOHNSON T. V. AND FANALE F. P. (1973) Optical properties of carbonaceous chondrites and their relationship to asteroids. *J. Geophys. Res.* **78**, 8507–8518.
- KELLER L. P. AND BUSECK P. R. (1990) Matrix mineralogy of the Lancelotti carbonaceous chondrite: A transmission electron microscope study. *Geochim. Cosmochim. Acta* **54**, 1155–1163.
- KING T. V. V. AND CLARK R. N. (1989) Spectral characteristics of chlorites and Mg-serpentine using high-resolution reflectance spectroscopy. *J. Geophys. Res.* **94**, 13 997–14 008.
- KNEŽEVIĆ Z. AND MILANI A. (1994) Asteroid proper elements: The big picture. In *Asteroids, Comets, Meteors 1993* (eds. A. Milani, M.

- Di Martino and A. Cellino.), pp. 143–158. Kluwer Academic Publishers, Dordrecht, The Netherlands.
- KROT A. N., PETAEV M. I., SCOTT E. R. D., CHOI B-G., ZOLENSKY M. E. AND KEIL K. (1998) Progressive alteration in CV3 chondrites: More evidence for asteroidal alteration. *Meteorit. Planet. Sci.* **33**, 1065–1085.
- LANDOLT A. U. (1973) UVB photometric sequences in the celestial equatorial selected areas 92–115. *Astron. J.* **87**, 959–1020.
- MCSWEENY H. Y., JR. (1977) Petrographic variations among carbonaceous chondrites of the Vigarano type. *Geochim. Cosmochim. Acta* **41**, 1777–1790.
- MORBIDELLI A., ZAPPALÀ V., MOONS M., CELLINO A. AND GONCZI R. (1995) Asteroid families close to mean motion resonances: Dynamical effects and physical implications. *Icarus* **118**, 132–154.
- NESVORNÝ D. AND MORBIDELLI A. (1998) Three-body mean motion resonances and the chaotic structure of the asteroid belt. *Astron. J.* **116**, 3029–3037.
- REINSCH C. H. (1967) Smoothing by spline functions. *Numer. Math.* **10**, 177–183.
- RIVKIN A. S. (1997) Observations of main-belt asteroids in the 3- μ m region. Ph.D. thesis, University of Arizona, Tucson, Arizona, USA. 163 pp.
- SCHERER P. AND SCHULTZ L. (2000) Noble gas record, collisional history, and pairing of CV, CO, CK, and other carbonaceous chondrites. *Meteorit. Planet. Sci.* **35**, 145–153.
- SCOTT E. R. D. AND JONES R. H. (1990) Disentangling nebular and asteroidal features of CO3 carbonaceous chondrite meteorites. *Geochim. Cosmochim. Acta* **54**, 2485–2502.
- TEDESCO E. F. (1994) Asteroid albedos and diameters. In *Asteroids, Comets and Meteors 1993* (eds. A. Milani, M. DiMartino and A. Cellino), pp. 55–74. Kluwer Academic Publishers, Dordrecht, The Netherlands.
- TEDESCO E. F., WILLIAMS J. G., MATSON D. L., VEEDER G. J., GRADIE J. C. AND LEBOFKY L. A. (1989) A three-parameter asteroid taxonomy. *Astron. J.* **97**, 580–606.
- TOMEOKA K. AND BUSECK P. R. (1990) Phyllosilicates in the Mokoia CV carbonaceous chondrite: Evidence for aqueous alteration in an oxidizing environment. *Geochim. Cosmochim. Acta* **54**, 1745–1754.
- VEEDER G. J., MATSON D. L., OWENSBY P. D., GRADIE J. C., BELL J. F. AND TEDESCO E. F. (1995) Eos, Koronis, and Maria family asteroids: Infrared (JHK) photometry. *Icarus* **114**, 186–196.
- WAHL W. (1950) The statement of chemical analyses of stony meteorites and the interpretation of the analyses in terms of minerals. *Mineral. Mag.* **29**, 416–426.
- WEISBERG M. K. AND PRINZ M. (1998) Fayalitic olivine in CV3 chondrite matrix and dark inclusions: A nebular origin. *Meteorit. Planet. Sci.* **33**, 1087–1099.
- WEISBERG M. K., PRINZ M., CLAYTON R. N. AND MAYEDA T. K. (1997) CV3 chondrites: Three subgroups, not two (abstract). *Meteorit. Planet. Sci.* **32** (Suppl.), A138–A139.
- ZAPPALÀ V., BENDJOYA Ph., CELLINO A., FARINELLA P. AND FROESCHLÉ C. (1995) Asteroid families: Search of a 12,487-asteroid sample using two different clustering techniques. *Icarus* **116**, 291–314.
- ZAPPALÀ V., CELLINO A., GLADMAN B. J., MANLEY S. AND MIGLIORINI F. (1998) Asteroid showers on Earth after family breakup events. *Icarus* **134**, 176–179.
- ZAPPALÀ V., BENDJOYA Ph., CELLINO A., DI MARTINO M., DORESSOUNDIRAM A., MANARA A. AND MIGLIORINI F. (2000) Fugitives from the Eos family: First spectroscopic confirmation. *Icarus* **145**, 4–11.
- ZELLNER B., THOLEN D. J. AND TEDESCO E. F. (1985) The eight-color asteroid survey: Results for 589 minor planets. *Icarus* **61**, 355–416.